Estimation of Shape Parameter for Generalized Gaussian Distributions in Subband Decompositions of Video

Kamran Sharifi and Alberto Leon-Garcia

Abstract—**A subband decomposition scheme for video signals, in which the original or difference frames are each decomposed into 16 equal-size frequency subbands, is considered. Westerink *et al.* [4] have shown that the distribution of the sample values in each subband can be modeled with a "generalized Gaussian" probability density function (pdf) where three parameters, mean, variance, and shape are required to uniquely determine the pdf. To estimate the shape parameter, a series of statistical goodness-of-fit tests such as Kolmogorov–Smirnov or chi-squared tests have been used in [4]. A simple alternative method to estimate the shape parameter for the generalized Gaussian pdf is proposed that significantly reduces the number of computations by eliminating the need for any statistical goodness-of-fit test.**

I. Introduction

Subband decomposition is used in video and image processing as a compression tool. The signal is decomposed into frequency subbands and each subband is encoded independently. In a lossy encoding scheme, the sample values in each subband, or their prediction errors after passing through a DPCM loop, are quantized. To design an appropriate quantizer, the distribution of the subband samples needs to be known [1]. It has been assumed that the probability density function of the subband values and their prediction errors is *Laplacian* [2], [3]. While this assumption seems more valid for the prediction errors of the sample values, the Laplacian distribution cannot adequately model the distribution of sample values.

Figs. 1 and 2 show the histograms of two subbands generated from the Flower sequence. The histogram of subband 2 of the original frame 1 and the histogram of subband 2 of the difference between frame 1 and frame 2 along with the Laplacian pdf's with the same mean and variance are shown, respectively. The mismatch between the test Laplacian pdf's and the actual histograms has also been observed for other test sequences.

Westerink *et al.* [4] have shown that the distribution of the sample values in each subband can be modeled with a generalized Gaussian pdf where three parameters, namely, mean, variance, and shape, are required to uniquely specify the analytic pdf. In this paper, we propose a simple method that enables us to find the best shape parameter for the generalized Gaussian distribution that best fits the data of each subband.

In Section II, the class of generalized Gaussian pdf's as the best candidate for this purpose is presented. To determine the best shape parameter for generalized Gaussian pdf, a simple method is developed in Section III. Section IV contains the simulation results and concluding remarks are presented in Section V.

II. Generalized Gaussian PDF

The class of *generalized Gaussian* probability distribution functions has been used in [4] to model the distribution of the subband values of images. It has been shown that this class of pdf's can

Manuscript received June 13, 1994; revised September 12 and October 24, 1994. This work was supported in part by the Canadian Institute for Telecommunications Research (CITR). This paper was recommended by Associate Editor Ming-Ting Sun.

The authors are with the Department of Electrical and Computer Engineering, University of Toronto, Toronto, Ont., Canada M5S 1A4.

IEEE Log Number 9407852.

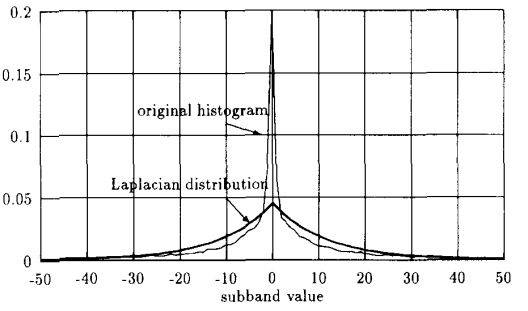

Fig. 1. The histogram of subband 2 of the original frame 1 of Flower sequence and its associated Laplacian distribution.

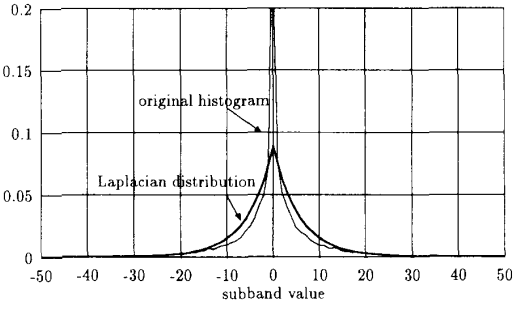

Fig. 2. The histogram of subband 2 of the difference between frames 1 and 2 of Flower sequence and its associated Laplacian distribution.

better match the real data than mere Laplacian pdf. The generalized Gaussian pdf [4], [5] is given by

$$f_X(x;\ \mu,\ \sigma^2,\ \gamma) = ae^{-[b|x-\mu|]^\gamma}, \qquad x \in \Re \tag{1}$$

where μ, σ^2, and γ are mean, variance, and shape parameter of the distribution, respectively. The positive constants a and b are given by

$$a = \frac{b\gamma}{2\Gamma(1/\gamma)}$$

and

$$b = \frac{1}{\sigma}\sqrt{\frac{\Gamma(3/\gamma)}{\Gamma(1/\gamma)}}$$

where $\Gamma(\cdot)$ is the Gamma function [6] given by

$$\Gamma(x) = \int_0^\infty t^{x-1}e^{-t}\,dt, \qquad x > 0. \tag{2}$$

The generalized Gaussian pdf is itself a generalization of a family of probability density functions called the *generalized Gamma* distributions, first introduced in [7]. The shape parameter γ in the generalized Gaussian pdf determines the decay rate of the density function. Note that $\gamma = 2$ yields the Gaussian (normal) density function and $\gamma = 1$ yields the Laplacian density function. The smaller values of the shape parameter γ correspond to more peaked distributions. Fig. 3 shows the generalized Gaussian distribution for three different shape parameters with the same variance.

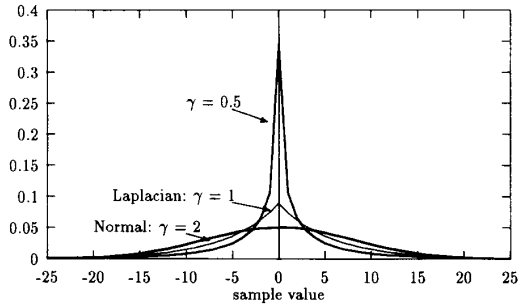

Fig. 3. Generalized Gaussian distribution for different shape parameters but with the same variance.

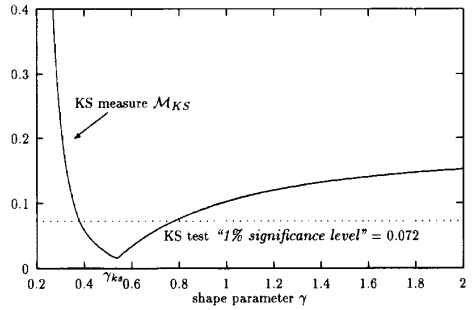

Fig. 4. KS test measures for subband 2 of frame 1 of Flower sequence.

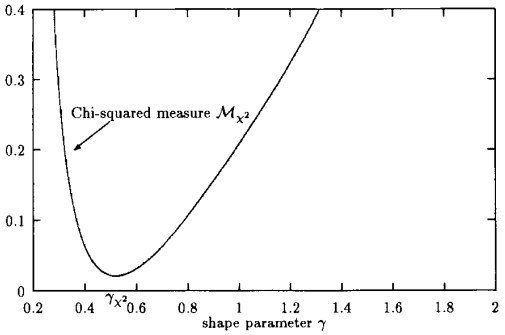

Fig. 5. Normalized χ^2 test measures for subband 2 of frame 1 of Flower sequence.

III. Modeling the Distribution of Values Using Generalized Gaussian PDF

We now try to match a given set of subband sample values with the best possible generalized Gaussian pdf. Equation (1) shows that three parameters, mean (μ), variance (σ^2), and shape (γ), are needed to fully determine the pdf.

The mean and the variance of the data are estimated using the following relations:

$$\hat{\mu}_X = \frac{1}{M}\sum_{i=1}^{M} x_i, \quad \hat{\sigma}_X^2 = \frac{1}{M}\sum_{i=1}^{M}(x_i - \hat{\mu}_X)^2 \tag{3}$$

in which x_i, $i = 1, \cdots, M$ is the subband sample value, M is the total number of samples in the subband, and $\hat{\mu}_X$ and $\hat{\sigma}_X^2$ are the mean and the variance estimates, respectively. Since M is large (on the order of 10^4 to 10^5), the estimates for mean and variance are precise enough. It now remains to estimate the shape parameter (γ).

Westerink *et al.* [4] have applied a series of statistical goodness-of-fit tests, specifically Kolmogorov–Smirnov (KS) and chi-squared (χ^2) [8], [9] to the experimental subband data to find the best value of the shape parameter for each subband.

In this method, the pdf (for χ^2 test) or the cumulative distribution function (cdf, for KS test) of one set of subband data are tested against a number of hypotheses. For each hypothesis, a generalized Gaussian pdf with a shape parameter γ chosen from the interval $[\gamma_{\min}, \gamma_{\max}]$ is postulated to fit the subband data. The mean and variance of all these pdf's are chosen to be $\hat{\mu}$ and $\hat{\sigma}^2$ which are the mean and variance estimate of the subband data, respectively. After performing both tests for different γ, the values of γ, for which the KS and χ^2 test measures are minimum (which we call γ_{KS} and γ_{χ^2} from this point on), are chosen as the best shape parameters for the generalized Gaussian pdf that fits the subband data.

Figs. 4 and 5 show the examples of the KS and χ^2 test measures for one set of subband data. Here we have chosen γ from the interval [0.2, 2.0] with step sizes equal to 0.01. This means that the subband data has been tested against 180 different hypotheses. The value of γ for which the KS test measure ($\mathcal{M}_{KS}$) is minimum is found to be $\gamma_{KS} = 0.54$. It is also shown that for this value of γ, the KS test measure (0.016) is less than the test 1% significance level (0.072) [8] (see Fig. 4). This observation, through KS test, approves the hypothesis that the experimental data can be modeled by a generalized Gaussian pdf with $\gamma = 0.54$. The same observations have been made by performing the χ^2 test that gives $\gamma_{\chi^2} = 0.53$ for the same set of data (see Fig. 5).

To derive the results of Figs. 4 and 5 and ultimately to find the best γ for one set of data, KS and χ^2 tests have been each applied to the actual data 180 times for 180 different hypotheses (180 different values of γ). This repetition of performing the statistical tests is the reason why this method is inherently very complex and needs a lot of computations.

We now develop a simple method that allows us to find the optimum shape parameter in one step, given the mean, variance, and the mean absolute value of the data. No goodness-of-fit tests or similar statistical measures will be used in the proposed method. As a result, the number of calculations to find the best pdf for the experimental data will be reduced drastically. The simplicity of the scheme is due to an explicit relation between the variance (σ_x^2), the mean of the absolute values ($E[|X|]$), and the shape parameter (γ) of a zero-mean generalized Gaussian pdf (see the Appendix):

$$r(\gamma) = \frac{\sigma_X^2}{E^2[|X|]} = \frac{\Gamma(1/\gamma)\cdot\Gamma(3/\gamma)}{\Gamma^2(2/\gamma)} \tag{4}$$

where $\Gamma(\cdot)$ is defined in (2). The function $r(\gamma)$, which we call the *generalized Gaussian ratio function*, is shown in Fig. 6 for $0 < \gamma \leq 2$.

We postulate that the pdf of any subband sample values can be fitted to a generalized Gaussian pdf with three unknown parameters: μ, σ^2, and γ. Our method works as follows:

1) Determine the estimate for the mean ($\hat{\mu}_X$) and variance ($\hat{\sigma}_X^2$) of the subband data based on (3).
2) Determine the estimate for the modified mean of the absolute values: $\hat{E}[|X|] = (1/M)\sum_{i=1}^{M}|x_i - \hat{\mu}_X|$.
3) Calculate the ratio $\rho = \hat{\sigma}_X^2/\hat{E}^2[|X|]$.
4) Find the solution to the equation $\hat{\gamma} = r^{-1}(\rho)$, in which r is the generalized Gaussian ratio function, defined in (4), by using a lookup table.

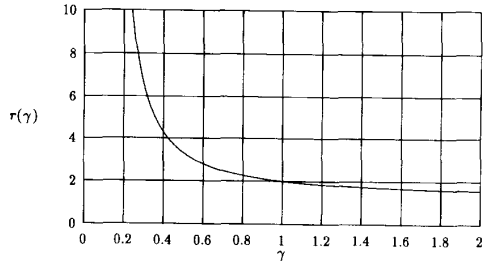

Fig. 6. The generalized Gaussian ratio function $r(\gamma)$.

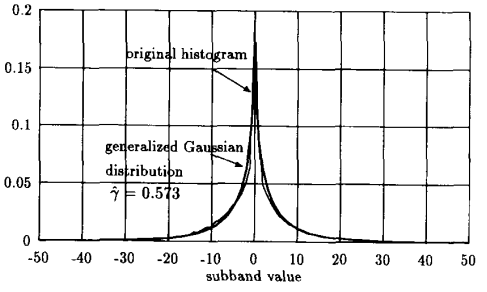

Fig. 7. Comparison of analytic distribution and actual histogram for subband 2 of the original frame 1 of Flower sequence.

With the determination of $\hat{\gamma}$ and having the sample mean $\hat{\mu}_X$ and variance $\hat{\sigma}_X^2$ for each subband, we can obtain the pdf that best matches the experimental histogram of the data in the form of (1).

IV. Simulation Results

We have used a two-stage filtering structure to decompose either the original or the difference frames of a video sequence into 16 equal-size frequency subbands [10]. The ratio $\rho = \hat{\sigma}_X^2/\hat{E}^2[|X|]$ has been obtained for each subband data. An estimate of the shape parameter $(\hat{\gamma})$ has been obtained by solving $\hat{\gamma} = r^{-1}(\rho)$ using a lookup table that stores the values of r for quantized values of γ. There are 180 entries in the lookup table for 180 different values of γ in the range of [0.2, 2.0] with a step size equal to 0.01. This range for γ was specifically chosen because in all cases, the shape parameters of the actual subband data of image and video fall in this range.

Our estimates of the shape parameter $(\hat{\gamma})$ are shown in Tables I–IV for all 16 subbands of some original and difference frames from the Flower, Tennis and Football sequences. Also in Figs. 7 and 8, the analytic pdf based on our estimate of shape parameter is shown along with the actual histogram for two sets of subband data.

To compare our estimate $\hat{\gamma}$ with the estimate given by the statistical tests, we have performed a series of goodness-of-fit test on each set of subband data to obtain γ_{KS} and γ_{χ^2} as defined in Section III. These results are also shown in Tables I–IV. The proximity of the results show the validity of our estimate of the shape parameter $(\hat{\gamma})$ with respect to the *best possible estimate* given by statistical tests (γ_{KS} and γ_{χ^2}).

In addition to comparing the results given by different methods, we have also tested all the experimental data using KS test against our hypothesis $\hat{\gamma}$. Table V shows the KS measures ($\mathcal{M}_{\mathrm{KS}}$) derived when a set of subband data is tested against two hypotheses: $\hat{\gamma}$ and γ_{KS}. Note that in all cases, the KS measure given by our hypothesis

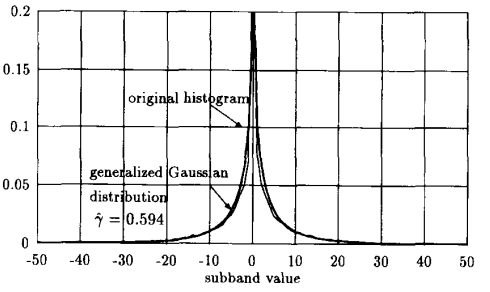

Fig. 8. Comparison of analytic distribution and actual histogram for subband 2 of the difference between frames 1 and 2 of Flower sequence.

TABLE I
Comparison of Optimum Shape Parameters Given by Three Methods for Flower

frame 1				frame 45			
subband	γ_{χ^2}	$\hat{\gamma}$	γ_{KS}	subband	γ_{χ^2}	$\hat{\gamma}$	γ_{KS}
1(DPCM)	.57	.61	.58	1(DPCM)	.67	.73	.69
2	.53	.57	.54	2	.56	.61	.57
3	.51	.52	.54	3	.61	.62	.62
4	.58	.58	.62	4	.67	.67	.68
5	.66	.66	.66	5	.63	.61	.62
6	.54	.55	.55	6	.58	.60	.60
7	.60	.61	.61	7	.71	.73	.71
8	.60	.60	.63	8	.68	.68	.69
9	.59	.53	.62	9	.68	.69	.76
10	.75	.75	.78	10	.80	.79	.82
11	.51	.43	.51	11	.53	.53	.55
12	.64	.64	.64	12	.71	.71	.71
13	.71	.65	.71	13	.80	.76	.79
14	.78	.79	.78	14	.87	.88	.88
15	.52	.53	.52	15	.62	.62	.61
16	.59	.62	.59	16	.69	.70	.70

TABLE II
Comparison of Optimum Shape Parameters Given by Three Methods for Football

frame 1				frame 45			
subband	γ_{χ^2}	$\hat{\gamma}$	γ_{KS}	subband	γ_{χ^2}	$\hat{\gamma}$	γ_{KS}
1(DPCM)	.53	.55	.55	1(DPCM)	.54	.56	.56
2	.74	.79	.73	2	.69	.68	.69
3	.57	.51	.55	3	.47	.48	.52
4	1.09	1.11	1.17	4	.74	.75	.76
5	.54	.50	.52	5	.37	.39	.39
6	.65	.65	.67	6	.42	.44	.47
7	.71	.68	.68	7	.40	.38	.40
8	.95	1.05	1.11	8	.80	.69	.74
9	.58	.50	.72	9	.63	.50	.74
10	1.10	1.61	1.68	10	1.01	1.06	1.05
11	.44	.46	.58	11	.43	.44	.55
12	1.30	1.34	1.37	12	.88	.80	.87
13	1.16	1.44	1.45	13	.91	.83	.86
14	1.09	1.69	1.54	14	1.11	1.23	1.15
15	1.30	1.10	1.23	15	.62	.45	.54
16	1.29	1.31	1.36	16	.74	.78	.89

$(\mathcal{M}_{\mathrm{KS},\hat{\gamma}})$ is less than the 1% significance level of the KS test (0.072) [8]. This observation has also been made for all other experimental data. In the same table, the KS test measures $(\mathcal{M}_{\mathrm{KS},\gamma_{\mathrm{KS}}})$ are given when the hypothesis γ_{KS} is tested by KS test. These are the minimum attainable KS test measures for that set of data.

TABLE III
COMPARISON OF OPTIMUM SHAPE PARAMETERS GIVEN BY THREE METHODS FOR TENNIS

frame 1				frame 28			
subband	γ_{χ^2}	$\hat{\gamma}$	γ_{KS}	subband	γ_{χ^2}	$\hat{\gamma}$	γ_{KS}
1(DPCM)	.75	.74	.78	1(DPCM)	.67	.68	.70
2	.62	.61	.62	2	.55	.54	.54
3	.93	.95	.96	3	.76	.78	.77
4	.92	.93	.93	4	.84	.84	.84
5	.40	.40	.47	5	.42	.40	.44
6	.51	.51	.58	6	.40	.40	.46
7	1.08	1.07	1.06	7	.98	.95	.97
8	1.05	1.05	1.06	8	.91	.91	.90
9	.91	.93	.91	9	.87	.81	.80
10	1.00	.99	1.01	10	1.11	1.06	1.06
11	.83	.82	.82	11	.72	.75	.75
12	.87	.86	.87	12	.86	.84	.84
13	.95	.95	.95	13	.93	.93	.95
14	1.02	1.01	1.02	14	1.10	1.08	1.09
15	.98	.98	1.01	15	.85	.86	.88
16	1.08	1.04	1.10	16	.91	.90	.92

TABLE IV
COMPARISON OF OPTIMUM SHAPE PARAMETERS GIVEN BY THREE METHODS FOR FLOWER, DIFFERENCE BETWEEN FRAMES 1 AND 2 AND FRAMES 44 AND 45

difference frame 1 & 2				difference frame 44 & 45			
subband	γ_{χ^2}	$\hat{\gamma}$	γ_{KS}	subband	γ_{χ^2}	$\hat{\gamma}$	γ_{KS}
1	.65	.67	.65	1	.62	.65	.63
2	.60	.59	.58	2	.61	.62	.63
3	.55	.55	.59	3	.63	.63	.64
4	.53	.58	.53	4	.67	.65	.69
5	.61	.63	.63	5	.57	.57	.57
6	.57	.59	.60	6	.62	.60	.60
7	.62	.61	.64	7	.72	.72	.71
8	.61	.59	.66	8	.66	.65	.68
9	.77	.77	.78	9	.84	.84	.84
10	.67	.69	.72	10	.78	.78	.81
11	.53	.51	.52	11	.54	.54	.56
12	.61	.63	.62	12	.67	.69	.71
13	.81	.80	.83	13	.85	.82	.86
14	.73	.74	.75	14	.82	.83	.84
15	.52	.51	.52	15	.57	.57	.56
16	.60	.61	.61	16	.67	.69	.69

V. CONCLUSIONS

The shape parameter of the generalized Gaussian pdf (γ) controls the shape (specially the peakedness) of the distribution and hence provides a degree of freedom to better match the actual distribution of the subband data over a broader range.

We developed a simple technique that allowed us to estimate the shape parameter (γ) in terms of the variance and mean absolute value of the data. We compared the results obtained by this simple technique with the results given by statistical goodness-of-fit tests. The simplicity of the method, compared to carrying out a series of statistical goodness-of-fit tests such as chi-squared or Kolmogorov–Smirnov, permits the fast characterization of the subband data distribution. The fast characterization of the distribution is essential in setting up an appropriate quantizer and hence stabilizing the end-to-end quality of the whole coding process.

APPENDIX

Let X be a generalized Gaussian random variable with the pdf given by (1). Without loss of generality, let $\mu = E[X] = 0$. We now show that there is an explicit relation between the variance σ_X^2 and the mean of the absolute values $E[|X|]$ under which we can write

$$\sigma_X^2 = r(\gamma)E^2[|X|]$$

where $r(\cdot)$ is a single-variable function of the shape parameter γ to be determined. To determine $r(\cdot)$, we start with the derivation of $E[|X|]$:

$$\begin{aligned} E[|X|] &= \int_{-\infty}^{+\infty} |x| f_X(x)\,dx \\ &= \int_{-\infty}^{+\infty} |x| a e^{-[b|x|]^\gamma}\,dx \\ &= \int_0^{\infty} 2axe^{-(bx)^\gamma}\,dx, \qquad (bx)^\gamma = y \\ &= \frac{2a}{b^2\gamma}\int_0^{\infty} y^{(2/\gamma-1)}e^{-y}\,dy \\ &= \frac{2a}{b^2\gamma}\Gamma\left(\frac{2}{\gamma}\right), \qquad 0 \le \gamma. \end{aligned} \tag{5}$$

The reader may note that the last step is due to the definition of Gamma function (2). Introducing a and b into (5) and after some manipulations yields

$$\sigma_X^2 = \frac{\Gamma(1/\gamma)\cdot\Gamma(3/\gamma)}{\Gamma^2(2/\gamma)}E^2[|X|]. \tag{6}$$

Equation (6) demonstrates the fact that the shape parameter for the generalized Gaussian distribution can be obtained in terms of the variance σ_X^2 and the mean absolute value $E[|X|]$. We call the function

$$r(\gamma) = \frac{\sigma_X^2}{E^2[|X|]} = \frac{\Gamma(1/\gamma)\cdot\Gamma(3/\gamma)}{\Gamma^2(2/\gamma)}$$

the *generalized Gaussian ratio function.*

TABLE V
KS TEST MEASURES DERIVED BY KS TEST WHEN EXPERIMENTAL DATA (FROM SUBBANDS OF FLOWER, FRAME 1) IS TESTED AGAINST TWO HYPOTHESES: $\hat{\gamma}$ AND γ_{KS}

subband	$\hat{\gamma}$	$\mathcal{M}_{KS}$ for hypothesis $\hat{\gamma}$	γ_{KS}	$\mathcal{M}_{KS}$ for hypothesis γ_{KS}
1	0.61	0.022	0.58	0.015
2	0.57	0.025	0.54	0.016
3	0.52	0.021	0.54	0.015
4	0.58	0.021	0.62	0.014
5	0.66	0.012	0.66	0.012
6	0.55	0.011	0.55	0.011
7	0.61	0.015	0.61	0.015
8	0.60	0.020	0.63	0.015
9	0.53	0.049	0.62	0.021
10	0.75	0.016	0.78	0.014
11	0.43	0.057	0.51	0.027
12	0.64	0.014	0.64	0.014
13	0.65	0.017	0.71	0.010
14	0.79	0.029	0.78	0.027
15	0.53	0.013	0.52	0.011
16	0.62	0.022	0.59	0.019

REFERENCES

[1] N. S. Jayant and P. Noll, *Digital Coding of Waveforms.* Englewood Cliffs, NJ: Prentice Hall, 1984.

[2] H. Gharavi and A. Tabatabai, "Subband coding of monochrome and color images," *IEEE Trans. Circuits Syst.*, vol. 35, pp. 207–214, Feb. 1988.

[3] J. W. Woods and S. D. O'Neil, "Subband coding of images," *IEEE Trans. Acoust., Speech, Signal Process.*, vol. ASSP-34, pp. 1278–1288, Oct. 1986.

[4] P. H. Westerink, J. Biemond, and D. E. Boekee, "Subband coding of color images," in J. W. Woods (Ed.), *Subband Image Coding.* Norwell, MA: Kluwer Academic, 1991.

[5] M. K. Varansai and B. Aazhang, "Parametric generalized Gaussian density estimation," *J. Acoust. Soc. Amer.*, vol. 86, no. 4, pp. 1404–1415, Oct. 1989.

[6] M. Abramowitz and I. A. Stegun, *Handbook of Mathematical Functions*. New York: Dover, 1970.
[7] E. W. Stacy, "A generalization of gamma distribution," *Ann. Math. Stat.*, vol. 28, pp. 1187–1192, 1962.
[8] A. O. Allen, *Probability, Statistics and Queueing Theory*. New York: Academic, 1978.
[9] A. Leon-Garcia, *Probability and Random Processes for Electrical Engineering*, 2nd ed. Reading, MA: Addison–Wesley, 1994.
[10] K. Sharifi, L. Xiao, and A. Leon-Garcia, "Adaptive subband coding of full motion video," in *Proc. SPIE Visual Commun. Image Process. '93*, vol. 2094, Nov. 1993, pp. 1390–1399.

An Adaptively Refined Block Matching Algorithm for Motion Compensated Video Coding

Yan Huang and Xinhua Zhuang

***Abstract*—An adaptively refined block matching algorithm (AR-BMA) for motion compensated (MC) video coding is presented. The AR-BMA algorithm requires transmitting the same amount of motion data as the conventional block matching algorithm (BMA) while achieving much higher prediction accuracy by an adaptive refinement scheme that captures the fine motion variations in video scenes. Experimental results show significant reduction of the prediction errors by the AR-BMA as compared with the full-search BMA.**

I. Introduction

Motion compensated (MC) video coding has received considerable attention in recent years for very low bit rate video compression. There are basically two groups of motion displacement estimation methods, namely, the block matching algorithms (BMA) and pel-recursive algorithms (PRA). The BMA partitions each image frame into a number of equal-sized blocks and finds a constant motion vector for each block by searching for its peak correlation with an associated block in the previous frame. Besides the full-search BMA, many fast algorithms such as the 2D-logarithm search (LOGS) [1], the three-step search [2] and its improvement [3], the cross-search algorithm [4], and the dynamic search-window adjustment algorithm [5] have been proposed to reduce the computational complexity. The full-search BMA, however, still enjoys its privilege for easy VLSI implementation and solution optimality [6], [7]. The advantages of the BMA's include computational regularity, robustness, as well as relative simplicity. Thus, the BMA's have become the baseline models in the MPEG recommendation for video coding standards [8]. Improvements over the BMA's by using more sophisticated models such as the hierarchical grid interpolation method [9] have also been investigated. On the other hand, the family of the PRA's are originated from the work of Netravali and Robbins [10] and improved for faster convergence and better stability [11], [12], [13]. In the PRA's, no motion vector needs to be transmitted and the motion compensation is accomplished by recursively updating the motion vectors from pixel to pixel in a causal order at both the encoder and decoder using the same algorithm. Nevertheless, the PRA's usually suffer from slow convergence and frequent divergence when applied on high motion video sequences. As a remedy, certain control strategies are often used to detect the divergence and reset the recursive procedure.

In this paper, we propose an adaptive refinement scheme to improve the motion data in the conventional BMA's. As is well known, the BMA's are based on the assumption that the motion displacement can be considered as constant in each given image block. This assumption, however, does not hold for large blocks, especially wherever motion boundaries are encountered. Although using relatively smaller matching blocks would often lead to more accurate motion estimates, it requires transmitting significantly more motion data, which is contradictory to the purpose of bandwidth reduction. In addition, small blocks contain less discriminative features so that false matches are more likely induced. Therefore, large blocks as 16×16 in size are used in most BMA's at the price of ignoring fine motion details. In order to recover the fine motion variations, we propose an adaptive motion refinement scheme to improve the motion data obtained in the BMA. In our scheme, the BMA is first performed on a large block base to obtain coarse but relatively reliable motion vectors, and then the local motion variation is adaptively captured on each pixel base by selecting an optimal refinement vector among those computed over a number of candidate masks in the small neighborhood. The proposed AR-BMA algorithm for MC video coding has the following features:

1) Without sending the refinement vectors, it requires transmitting only the same amount of motion data as in the conventional BMA's.
2) It has the similar effect in accounting for fine motion variations as the block matching that uses small blocks; but it does not suffer much the false matching problem since the motion vectors are refined based on the relatively reliable initial estimates.
3) At the refinement stage, no time-consuming searching process is performed for finding the best match; instead, a motion refinement model is used to uniquely determine the solution in subpixel accuracy.
4) The algorithm combats many practical problems caused by image noises or slight violations of some commonly used assumptions.

II. Adaptive Motion Refinement Scheme

Block matching is first performed between the $(k-1)$th frame, f_{k-1}, and kth frame f_k by using the following mean-squared errors (MSE) criterion to find a constant integer vector $\boldsymbol{d}^0$ for each large matching block $\mathcal{N}$,

$$\boldsymbol{d}^0 = \arg\min_{\boldsymbol{d}} \sum_{z_i \in \mathcal{N}} |f_k(z_i) - f_{k-1}(z_i - \boldsymbol{d})|^2. \tag{1}$$

where z_i denotes the i-th pixel. Suppose the initial motion vectors (one for each block) and the pixels preceding the current pixel z_n have all been transmitted to the decoder. Let $\boldsymbol{d}_n^0$ be the initial motion vector for pixel z_n, and $\boldsymbol{d}_n$ be the true motion vector

$$\boldsymbol{d}_n = \boldsymbol{d}_n^0 + \boldsymbol{\delta}_n. \tag{2}$$

It is common to assume that the image intensity remains unchanged along the motion trajectory, i.e.,

$$f_k(z_n) = f_{k-1}(z_n - \boldsymbol{d}_n). \tag{3}$$

Manuscript received August 10, 1994; revised October 18, 1994. This paper was recommended by Associate Editor Ming T. Sun.

The authors are with the Department of Electrical and Computer Engineering, University of Missouri, Columbia, MO 65211, USA.

IEEE Log Number 9407821.